Per. Mineral. (2002), *71*, SPECIAL ISSUE: *Archaeometry and Cultural Heritage*, **73-85** http://go.to/permin

PERIODICO di MINERALOGIA
established in 1930

An International Journal of
MINERALOGY, CRYSTALLOGRAPHY, GEOCHEMISTRY, ORE DEPOSITS, PETROLOGY, VOLCANOLOGY
and applied topics on *Environment, Archaeometry* and *Cultural Heritage*

Combined Microanalytic and Electron Paramagnetic Resonance techniques in archaeometry of ancient glass from Lomello (Pavia, northern Italy).

CARLO B. AZZONI[1], DANIELA DI MARTINO[1], BRUNO MESSIGA[2]* and MARIA P. RICCARDI[2]

[1] INFM - Dip. Fisica «A. Volta», Università di Pavia, Via Bassi 6, I-27100 Pavia, Italy
[2] Dip. Scienze della Terra, Università di Pavia, Via Ferrata 1, I-27100 Pavia, Italy

ABSTRACT. — The combined use of Electron Microprobe (EMP) and Electron Paramagnetic Resonance (EPR) was applied to the characterisation of ancient glass. The resulting data were complementary and thus very useful for information on both glass composition and the oxidation state of paramagnetic ions, such as Fe^{3+} and Mn^{2+}. Our study highlighted the importance of obtaining the abundances (EMP) and oxidation states of the above elements (EPR). These indications represent a new way of looking at ancient glass production and may define several production indicators such as control of kiln atmosphere. Our results show that the value of the oxidising/reducing ratio defines a parameter constraining the colour of worked glass - an aspect which has implications for archaeometric research aiming at reconstructing the history of glass.

RIASSUNTO. — Tecniche di microanalisi (EMP) e di risonanza paramagnetica elettronica (EPR) sono state utilizzate congiuntamente per la caratterizzazione di vetri antichi. I dati raccolti sono risultati tra loro complementari, e quindi preziosi, nel fornire informazioni sulla composizione del materiale e sullo stato di ossidazione di ioni paramagnetici, quali Fe^{3+} e Mn^{2+} presenti nei campioni esaminati. Lo studio ha messo in evidenza l'importanza di ottenere dati relativi alle quantità e allo stato di ossidazione di Ferro e Manganese. Tali dati possono rappresentare un nuovo modo di studiare la produzione di vetri nell'antichità, ed in particolare per definire indicatori di produzione relativi al controllo della atmosfera del forno. I risultati ottenuti permettono di definire i valori del rapporto ossidante/riducente che determina il colore di vetri lavorati. Questo aspetto ha implicazioni nelle ricerche storiche ed archeometriche sul vetro antico.

KEY WORDS: *Ancient glass, Electron Microprobe, Electron Paramagnetic Resonance, colour attributes, redox ratio.*

INTRODUCTION

In Roman times, Lomello, near Pavia, in northern Italy, was an important settlement along one of the main roads leading to Gaul (Blake and Maccabruni, 1985; Blake *et al.*, 1987). During archaeological excavations, glass artefacts were found in such significant quantities that they could be used to investigate such materials over a period of time from Roman times to the Middle Ages. Time relationships were deduced from their association with pottery fragments (Blake *et al.*, 1987).

The relative abundances and the size of some fragments allowed mg in weight to be applied to many samples. Among these, a series of glass samples was characterised by combined use of the Electron Microprobe (EMP) and Electron Paramagnetic Resonance (EPR).

EMP is a widespread technique commonly used in Earth and Material Sciences to characterise phase composition by «spot»

* Corresponding author, E-mail: messiga@crystal.unipv.it

analysis (beam size less than 10 μm). The analytical method defines major element abundances (higher than 0.1 wt% in oxide). No element valence can be detected by this method.

EPR is a specific and highly sensitive technique for the characterisation of paramagnetic ions, even at very low concentrations. Many studies followed the first application of EPR to glass in 1955 (Griscom, 1980, and references therein). Due to the absence of any long-range order inside glass structures, the EPR signal of amorphous materials is more difficult to interpret than that of crystalline samples. In any case, some oxidation states can easily be detected (e.g., Fe^{3+}, Mn^{2+}, Mn^{4+}, Cu^{2+} ions) and additional indications derived through EMP can be supplied: chemical analysis can derive only elemental concentrations, whereas EPR can detect different valence states. Thus, a combination of these differing techniques is useful in characterisation of glass samples.

Investigations of ancient glass artefacts have so far mainly been carried out on bulk chemistry data (Brill, 1992, 1999; Amrein *et al.*, 1995; Cesana *et al.*, 1996; Fiori and Macchiarola, 1996; Ruffini *et al.*, 1999 a, b). Recent papers (e.g., Messiga and Riccardi, 2001) have emphasised how relationships between microtextures and micro-analyses are useful in unravelling ancient technological expedients used in glass production.

This paper reports a first attempt at archaeometric characterisation of ancient glass using combined microtextural, microchemical (EMP) and EPR analyses. Several glass samples from the archaeological site of Lomello were analysed: i) dark brown glass cake (VM1210/1), (XII century); ii) two vitreous masses (US3358a, US3358b), light blue and blue in colour (I-IV centuries A.D.); iii) five transparent worked glass pieces, colourless (US1754, US3122/89), pale blue (US1744) or green (US1684, US1611). The ages of these samples span the V-VII centuries and the XII century A.D..

The aim of our study was to verify how combined EMP and EPR analyses can help solve problems in setting the kiln atmosphere in order to obtain particular glass features (e. g., colour attributes).

METHODS AND TECHNIQUES

This study combines analytical data produced with bulk and «in situ» techniques. Bulk analyses were produced by X-ray fluorescence (XRF) and EPR. EMP was employed for micro-analyses. Microtextural examination under optical (OM) and scanning electron microscopes (SEM) was also essential to define microtextures on different observation scales.

The analytical data were obtained with the following instruments:

– XRF: Philips PW 1480, Rh and W tubes, according to the element analysed, in the 1600-3000 V range.

– EPR measurements: carried out at room temperature, with a Bruker spectrometer at 9.28 GHz (X band). All EPR spectra were normalised to the same weight and sensitivity. No special treatment of samples was required, the only insignificant limitation being maximum sample size (3 mm diameter, 20 mm length). Modern samples, used as references in data analysis, were soda-lime glass with known additions of single oxides, in particular: 0.15%, 1% Fe_2O_3, 1% and 2% MnO (see Chiavari *et al.*, 2001, for details). The sample with only 0.15% Fe_2O_3 gave an intense EPR signal, the detection limit being approximately 0.1 ppm.

– EMP and SEM: JEOL JXA 840A electron microanalyzer equipped with three wavelength dispersive spectrometers (TAP, PET and LIF analysing crystals) and one Si(Li) energy-dispersive spectrometer (Be window). Analytical conditions of 20kV accelerating voltage and 20 nA were employed, with a spot size of 5 μm. Data collected by the WDS were processed with the TASK correction program. Mineral phases were used as standards, to avoid matrix effects. Estimated precision was about 3% for major and 10% for minor elements, respectively.

RESULTS

Archaeological artefacts

Eight samples from three different types of findings were analysed (Fig. 1). A detailed description of textures and related compositions is given in Messiga and Riccardi (2001).

The vitreous masses are composed of dusted glass with ribbon-textured, yellowish and darker reddish-brown bands (Fig. 2A). Colourless glassy portions are not widespread (less than 5% vol). Darker bands have variable thickness and represent 20-25% of the vitreous mass volume (Fig. 2B). These masses also display some Fe-P alloy inclusions (about 100μm wide), new phase crystallisation (wollastonite, akermanite) and partially melted minerals. The cake has a ribbon texture, and crystalline phases are widespread (Fig. 2C). The ribbon texture is inhomogeneously distributed within the body; bands of different thickness are generally bent or folded. The worked glass is homogeneous, dense, transparent and colourless or weakly coloured, with trails of micro-bubbles (5-100 μm in size). Examples of micro-creep are widespread along the surfaces and closely related to alteration processes spreading into the glass (Fig. 2D). Sequences of edges in a concentric arrangement are due to secondary weathering during burial.

Composition

Glass composition is shown in the conventional ternary diagram (Fig. 3), commonly used to derive straightforward relationships between compositions, ages and recipes (Gratuze *et al.*, 1997; Moretti, 2000). Comparisons between bulk and «in situ» analyses reveal that: i) «in situ» analyses display a larger compositional range, reflecting the inhomogeneity of the glass; ii) bulk analyses have no baricentric position (mean value) in the compositional field defined by EMP analyses.

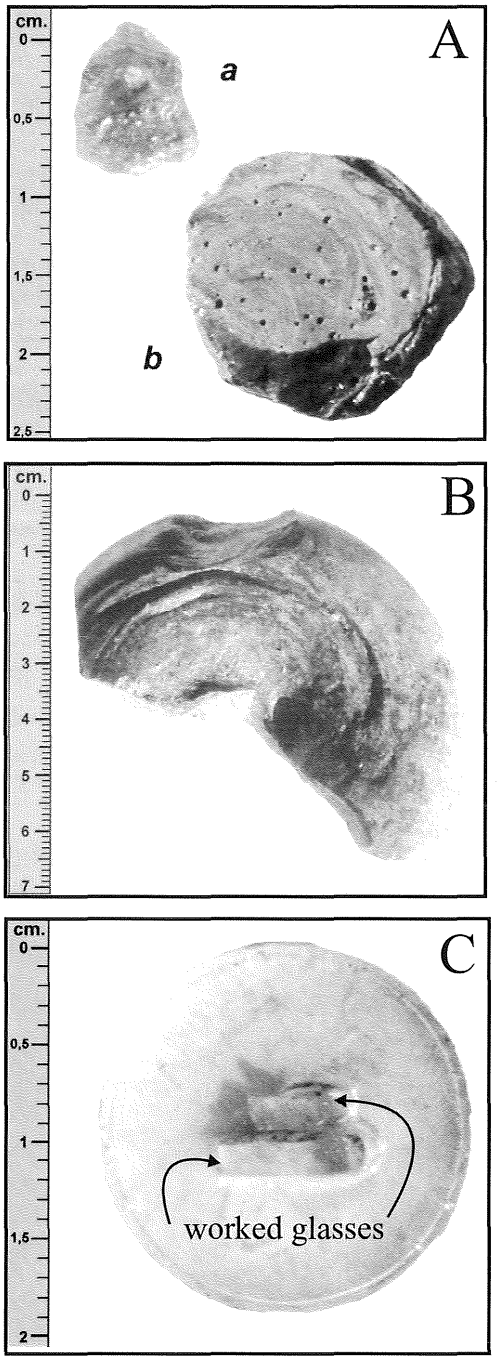

Fig. 1 – Different types of archaeological artefacts: A – vitreous masses; B – cake; C – worked glass.

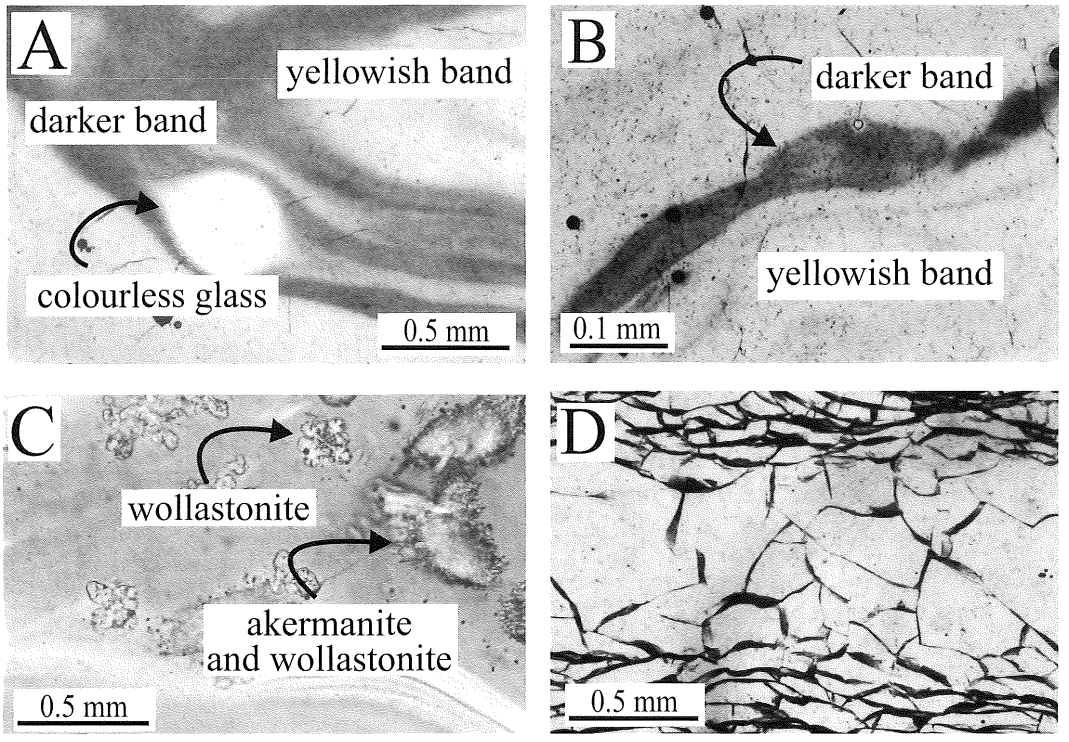

Fig. 2 – Textural details of glass artefacts. A – ribbon texture and colourless glass of vitreous masses; B – darker bands in vitreous masses; C – ribbon texture and crystalline phases in cake; D –homogeneous texture of worked glass.

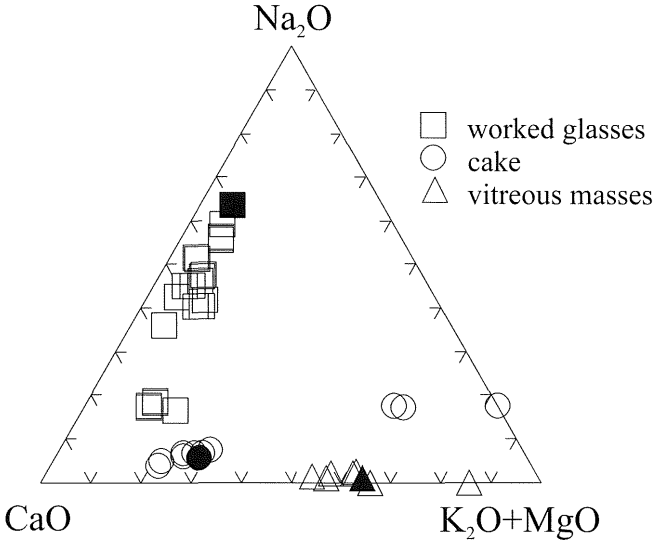

Fig. 3 – Conventional ternary plot CaO-(K_2O+MgO)-Na_2O (Gratuze *et al.*, 1997; Moretti, 2000). Full symbols: XRF data.

The worked samples are Na-glass, except for sample 1611, which has low contents of Na_2O; the other artefacts are Ca (Mg)-K-glass. Each sample type shows marked chemical differences when bulk (XRF) or micro-analyses (EMP) are considered, shown in Tables 1 and 2, respectively.

Abundances of vitrifying, stabilising and fluxing agents are shown in Figure 4. V*itrifying agents* (Al_2O_3, SiO_2) (Fig. 4A) are the network-forming components (Newton and Davison, 1997). Worked glass has the highest SiO_2 content; the cake and vitreous masses show SiO_2 less than 70 wt%, whereas Al_2O_3 ranges between 5 and 20 wt%. Two distinct glass compositions characterise cake and vitreous masses: most of the body (higher than 75% vol.) clusters in a field with lower SiO_2 content. In the cake, Al_2O_3 is slightly higher than in the vitreous masses. Other compositions regard inhomogeneities present in both types. In terms of *stabilising agent* abundance (CaO, MgO) (Fig. 4B), the worked glass is the most homogeneous, MgO and CaO contents ranging between 0.5-2 wt% and 15-20 wt%, respectively. Vitreous masses and cake display two distinct values for the MgO/CaO ratio: 0.4 and 0.2 respectively. *Fluxing agent* content ranges widely (Fig. 4C). The worked glass is Na-bearing, with Na_2O contents of up to 15wt%. The compositional range is due to differences in analysed samples. The cake contains K_2O up to 12wt% and the vitreous masses up to 20wt%. Fig. 4 also shows the bulk composition of artefacts obtained by XRF:

TABLE 1

XRF data (only major elements) for three types of studied samples. Values refer to worked glass and are averages of all samples.

	worked glasses	vitreous masses	cake
SiO_2	69.29	51.43	49.98
TiO_2	0.13	0.49	0.29
Al_2O_3	2.30	8.67	4.71
Fe oxides	1.40	11.49	2.78
Mn oxides	0.45	0.39	0.16
MgO	0.78	3.60	5.04
CaO	6.96	17.03	14.02
Na_2O	17.85	1.51	0.33
K_2O	0.62	3.90	20.27
P_2O_5	0.22	1.51	2.42
tot wt%	100.00	100.02	100.00

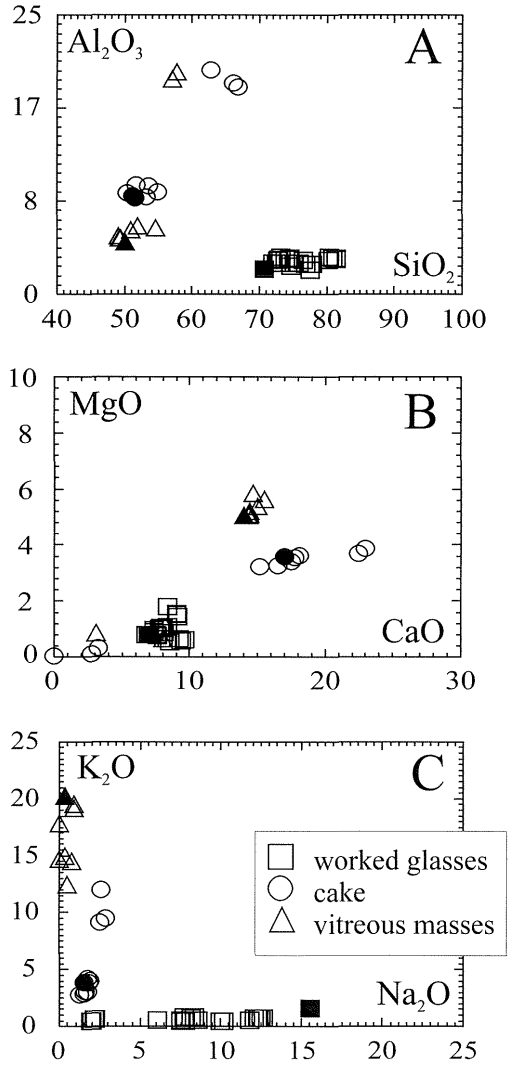

Fig. 4 – In situ analyses (EMP). A – vitrifying agents; B – stabilising agents; C – fluxing agents. See text for more details. Full symbols: XRF data.

TABLE 2

EMP data. Each column represents average of five EMP microanalyses; for cake and vitreous masses, compositions of glass unhomogeneities are also listed.

	worked glasses					cake		vitreous masses	
sample	US1611	US3122/89	US1684	US1754	US1744	Ca-K-glass	Al-glass	colourless glass	Ca-glass
SiO_2	80.88	74.43	72.75	73.84	75.47	50.80	57.46	65.24	52.34
TiO_2	0.28	0.10	0.19	0.20	0.19	0.46	0.04	0.07	0.56
Al_2O_3	3.21	3.05	2.79	3.23	3.07	5.49	19.57	19.16	9.10
Cr_2O_3	0.04	0.02	0.01	0.03	0.02	0.01	0.00	0.01	0.04
Fe oxides	1.14	0.45	1.02	1.12	0.93	2.27	0.39	0.47	8.33
Mn oxides	1.30	2.19	0.75	1.98	1.55	0.08	0.01	0.03	0.56
MgO	1.04	0.61	1.04	1.50	1.05	5.45	0.75	0.17	3.52
CaO	7.99	9.02	7.90	9.07	8.49	14.78	5.56	2.02	18.63
Na_2O	2.08	8.53	12.38	7.82	7.70	0.70	0.00	2.64	1.64
K_2O	0.52	0.51	0.74	0.72	0.62	16.71	16.28	10.21	3.43
P_2O_5	0.00	0.00	0.00	0.00	0.00	3.28	0.00	0.00	0.00
Cl*	1.54	1.09	0.43	0.49	0.89	0.00	0.00	0.00	1.67
Tot (wt%)	100.00	100.00	100.00	100.00	100.00	100.02	100.05	100.01	99.83

the figure represents mean sample compositions, but does not give information on compositional variabilities.

Additives such as Mn and Fe oxides have different abundances for different sample types, and the compositional range within a given sample (e.g., worked glass) is similarly wide (Fig. 5A). Vitreous masses and cake have Mn oxide content invariably lower than 1wt%; there is a correlation between Fe and Mn oxides only for the blue vitreous masses. The cake also reveals an appreciably high P_2O_5 content (up to 4wt%). Figure 5B shows that the colourless worked glass has more Mn oxides than the green and pale blue samples (Mn oxide up to 1wt%).

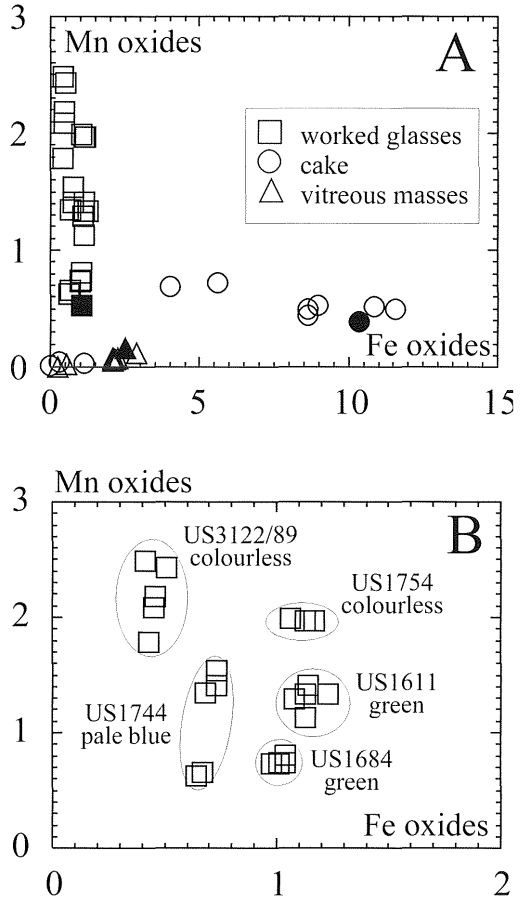

Fig. 5 – In situ analyses (EMP) of iron and manganese contents (A), with a detail of worked glass (B). Full symbols: XRF data.

EPR results

EPR spectra (Fig. 6) were interpreted as the sum of an asymmetric signal at g~2 and an asymmetric one at g~4.3, both attributed to Fe^{3+} and Mn^{2+} ions, as evidenced by comparison with the reference glass samples, with known additions of MnO and Fe_2O_3.

The EPR spectrum from Fe^{3+} ions consists of a sharp resonance peak at g~4.2 (narrowing as Fe^{3+} concentration decreases) and a broad band around g~2. The commonly accepted interpretation is that low symmetry sites of either tetrahedral or octahedral coordination give rise to g~4.2 resonance whereas, at higher Fe^{3+} concentrations, both coordinations also give rise to g~2 resonance (Griscom, 1980). The EPR spectrum attributed to the Mn^{2+} ion has a resonance peak at g~4.3 (shifted, broader, and less intense than the corresponding Fe^{3+} one) and a band at g~2 (narrower and more intense). No ^{55}Mn hyperfine structure, with nuclear spin of 5/2 and 100% abundance, is usually resolved for concentrations higher than 0.1% Mn^{2+} (Abidi *et al.*, 1997).

Figure 7 shows two examples of comparisons between Lomello and reference samples. The cake (sample VM1210/1) has very low Fe^{3+} and Mn^{2+} is nearly absent. Its EPR spectrum clearly overlaps that of the reference sample containing 0.15wt% Fe_2O_3, indicating that no more than 0.15wt% Fe^{3+} can be present in the cake (perhaps less, since 0.15wt% represents total iron ions). Worked glass sample US3122/89, in which the sharp Fe^{3+} signal is less evident, was also compared with the reference sample with 1 wt% MnO and the resulting concentration in the sample was 2.4wt% of Mn^{2+}.

Assuming that, with low manganese and iron contents, the EPR spectra linearly change with concentration, the EPR signals were resolved into Mn^{2+} and Fe^{3+} components. Samples US3358a and US5358b (vitreous masses) show deviations from baseline, probably due to

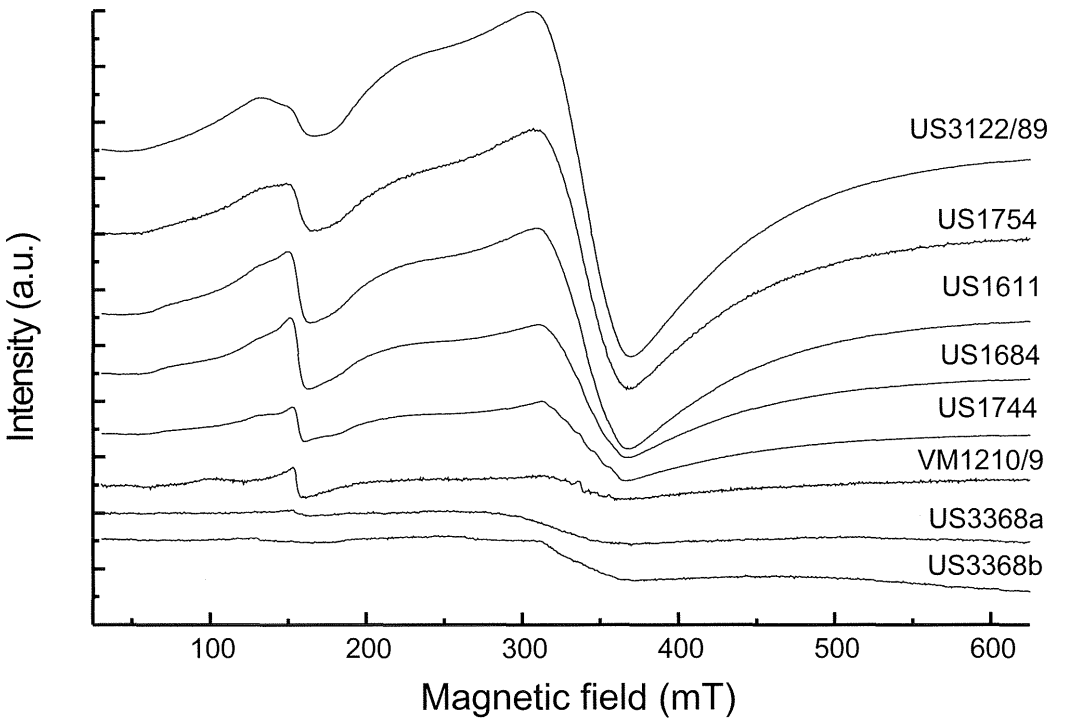

Fig. 6 – EPR spectra (normalised to weight and sensitivity).

TABLE 3

Worked glass: contents and oxidation states for iron and manganese, obtained by EMP and EPR analyses.

	US1744 V century AC pale blue	US3122/89 no data colourless	US1754 VII century AC colourless	US1684 VII century AC green	US1611 XII century AC green
Fe oxides	1.03	0.50	1.27	1.13	1.27
Fe_2O_3	0.18	0.05	0.23	0.40	0.37
FeO	0.76	0.40	0.92	0.66	0.81
Mn oxides	1.55	2.19	1.98	0.76	1.30
MnO	0.32	2.40	1.54	0.56	1.08
Mn_2O_3	1.51	0.00	0.54	0.24	0.12
Fe^{2+}/Fe^{3+}	4.22	8.00	4.00	1.65	2.19
Mn^{2+}/Mn^{3+}	0.21	0.00	2.85	2.33	10.00
Fe^{2+}/Mn^{2+}	2.38	0.17	0.60	1.18	0.68
Fe^{3+}/Mn^{3+}	0.12	0.00	0.43	1.67	3.08

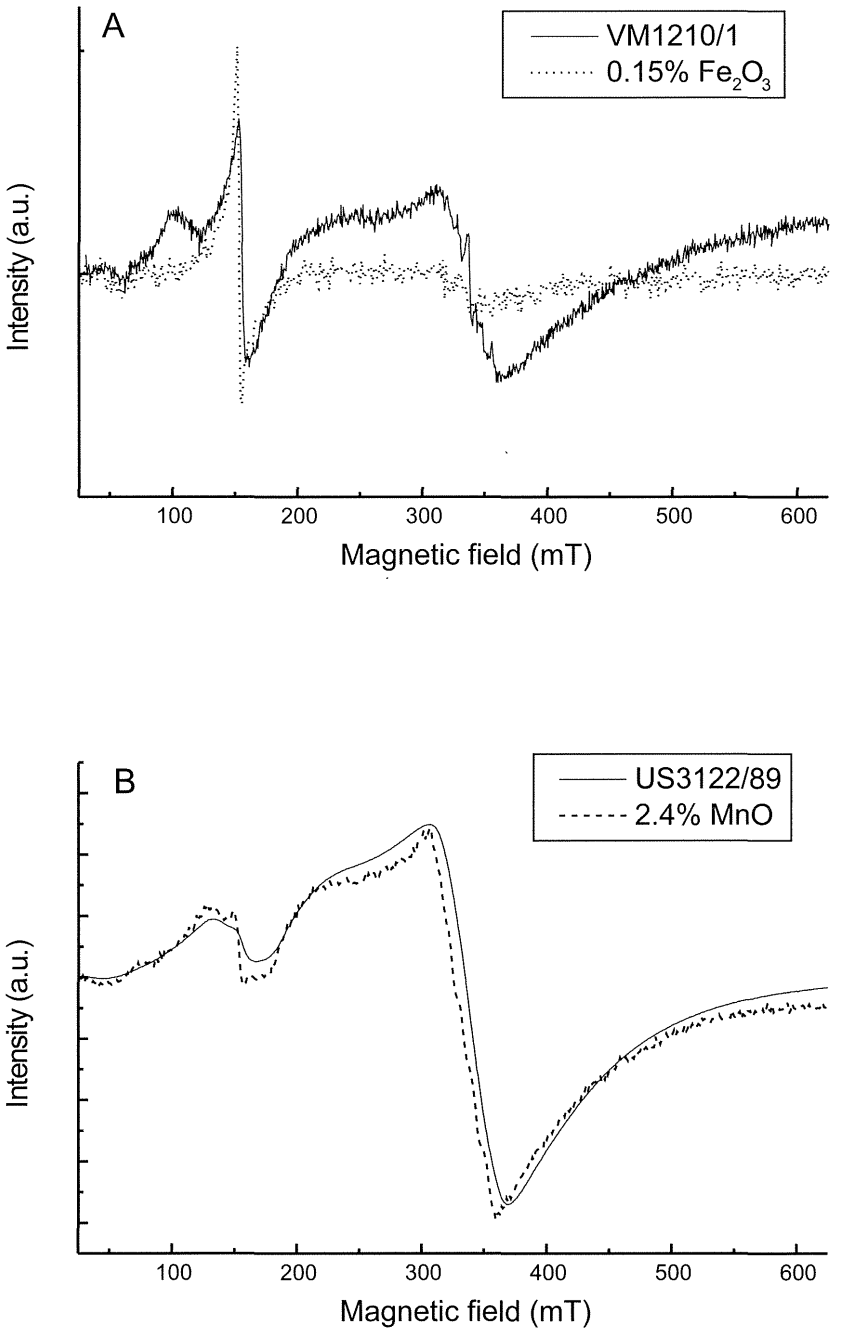

Fig. 7 – Comparisons between EPR spectra. (A) sample VM1210/1 (solid line) compared with reference sample containing 0.15 wt% Fe_2O_3; (B) sample US3122/89 (solid line) compared with 2.4 times reference sample containing 1 wt% MnO.

organic contaminants. The following Fe^{3+} (as Fe_2O_3) concentrations were derived for the worked glass samples: US1684: 0.40wt%; US1611: 0.37wt%; US1754: 0.23wt%; US1744: 0.18wt% and US3122/89: 0.05wt% (Tab. 3).

Concerning Mn^{2+} (as MnO) contents, the following indications were obtained: sample US1684: 0.56 wt%; sample US1744: 0.32 wt%; sample US1611: 1.08 wt%; sample US1754: 1.54 wt%; sample US3122/89: 2.40 (Tab. 3).

An overall EPR picture is shown in Figures 8 and 9, for Fe^{3+} and Mn^{2+} signals respectively. All samples show signals for Fe^{3+} and Mn^{2+}, although considerable differences in concentration are apparent.

Samples US3358a and US5358b both show a Mn^{2+} signal (< 0.1 wt%), whereas only sample US3358a shows a recognisable concentration (< 0.15 wt%) of Fe^{3+}. In sample US3358b, the narrow signal component detected at g~<2 may be due to the presence of Mn^{4+}, thus explaining the difference in colour between the two samples. In effect, inhomogeneity in concentration and valence of chromophore elements may arise as a result of different local reactions to firing in the same vitreous mass.

DISCUSSION AND CONCLUSIONS

The Na-bearing and Ca-Na-bearing worked glass samples display textural and compositional homogeneity in major element

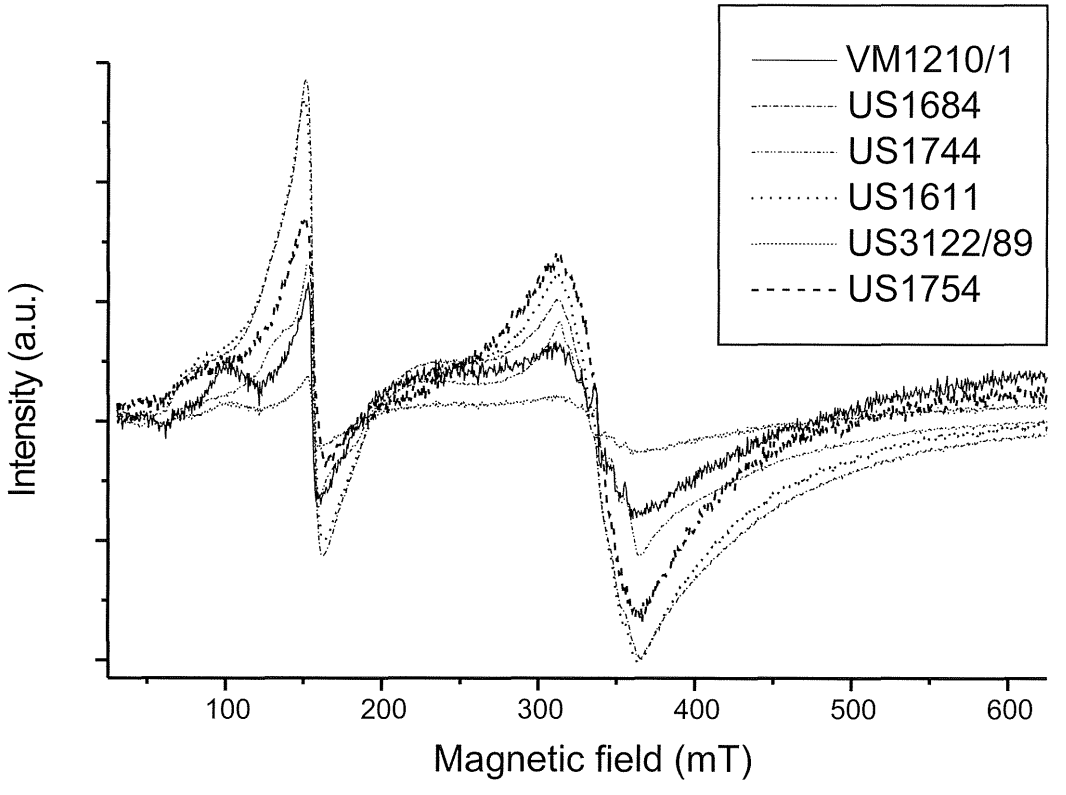

Fig. 8 – EPR spectra, amplified four times, resolved into Fe^{3+} content.

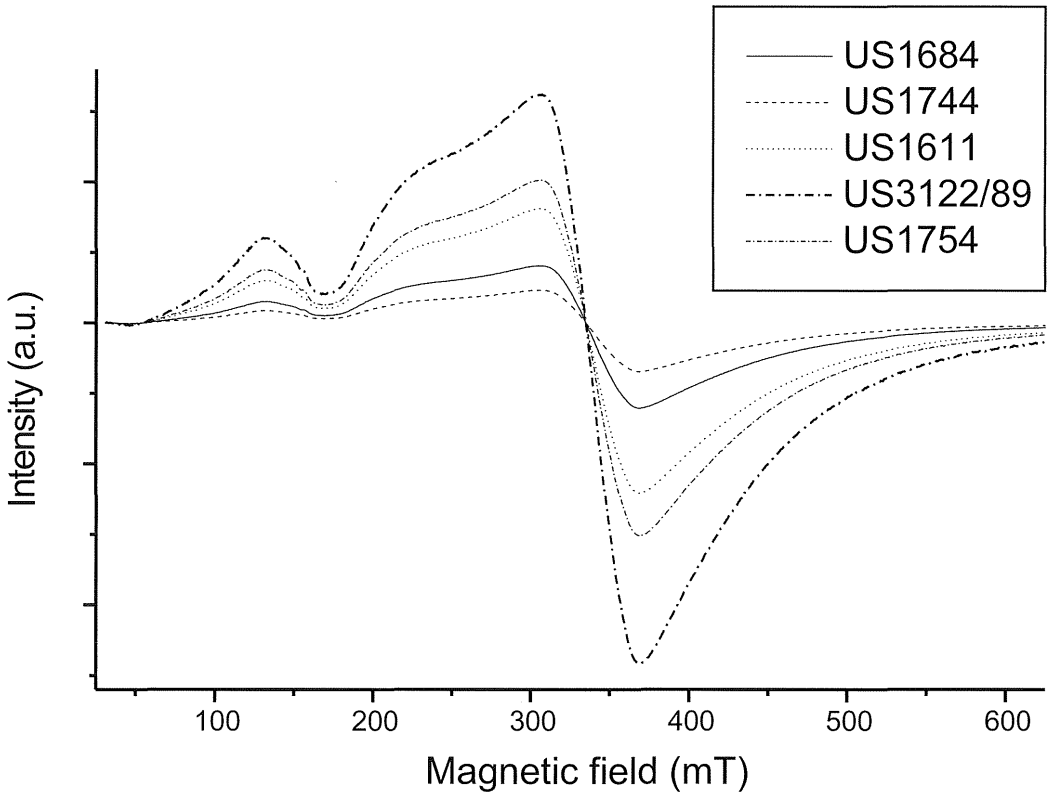

Fig. 9 – EPR spectra resolved into Mn^{2+} content.

abundances. The Ca-bearing vitreous masses and Ca-K-bearing cake are compositionally inhomogeneous, due to their ribbon texture, mineral/glass inclusions and phase immiscibility (Messiga and Riccardi, 2001). The ribbon texture indicates that complete mixing of two separate glass compositions was not achieved. The worked glass samples have has a more homogeneous composition, resulting from a careful fining process, and for this reason were more suitable for comparing EPR and EMP analyses.

Concerning EPR data, all samples exhibit signals attributed to different concentrations of Fe^{3+} and Mn^{2+}. There are important differences between EPR and XRF micro-analyses. For example, in the cake no more than 0.15 wt% Fe^{3+} was deduced by EPR, whereas the XRF found around 2.78 wt% Fe oxides. Thus, a meaningful concentration of Fe^{2+} (for which EPR signal is undetectable in glass) is probably present in that sample. This fact is explained by the compositional inhomogeneity of the sample, as detected by microtextural analysis.

Table 3 summarises values for iron and manganese abundances, as obtained from EMP and EPR analyses in worked glass samples. EPR supplies possible abundances for Fe_2O_3 and MnO; consequently, the ratio between Fe^{2+}/Fe^{3+} and Mn^{2+}/Mn^{3+} may be calculated. The state of oxidation in a kiln determines the above ratio and is responsible for the colour produced in Mn-Fe-bearing glass. This implies that an equilibrium reaction between the

different states of oxidation of manganese and iron is related to the kiln atmosphere during melting process, according to the equation:

$$Fe^{2+} + Mn^{3+} <==> Fe^{3+} + Mn^{2+}$$

Both Fe^{3+} and Mn^{2+} are more stable states, and hence the equilibrium tends to move to the right. Thus, when melting occurs in reducing conditions, equilibrium is forced to the left. Fe^{2+} ions contribute to a bright blue colour and Mn^{3+} does not make any chromatic contribution, so that a blue glass is obtained. When conditions are fully oxidising, Fe^{3+} contributes a brownish colour and Mn^{2+} purple, so that the glass appears brownish-violet. When conditions are intermediate, a different colour is obtained, including colourless glass (Sellner, 1977; Sellner and Camara, 1979; Triscari *et al.*, 2000).

In our samples, the lowest Fe^{3+}/Mn^{3+} ratio (< 1.0) occurs in the colourless glass (Fig. 10A) and is due to a higher Fe^{2+}/Fe^{3+} ratio (Tab. 3). The pale blue glass has the highest Fe^{2+}/Mn^{2+} ratio. Green worked glass always has Fe^{3+}/Mn^{3+} values above 1. Moreover, the highest Fe^{2+}/Fe^{3+} ratios are related to the highest Mn oxide contents (Fig. 10B).

It was noted that Mn oxides/Mn^{2+} values decrease in the increasingly younger artefacts.

The EMP technique provides spot analyses necessary to infer glass processing. This may be achieved when microprobe analyses are carried out on microtextures indicating a specific operation (e.g., blending of recycled glass, mineral phases present within the batch, phase separation due to crystallisation). However, no information is available on the oxidation state of elements by microprobe analysis, which prevents knowledge of details of kiln atmosphere composition.

The EPR technique is very suitable for comparative evaluations of the oxidation state, mainly of iron and manganese ions. The combined use of EPR and microprobe analysis gives complete compositional information: nominal compositions (derived through microprobe analysis) and relative redox ratios (derived through EPR).

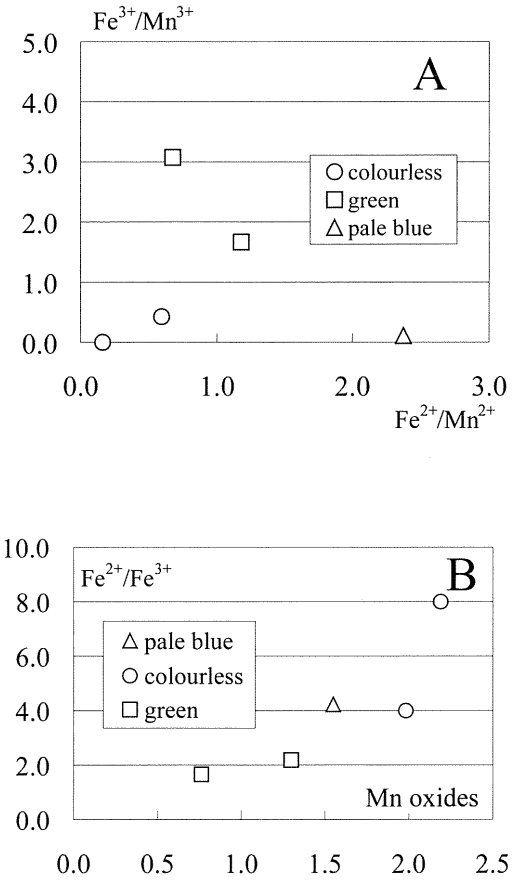

Fig. 10 – Fe^{3+}/Mn^{3+} and Fe^{2+}/Fe^{3+} ratios in worked glass samples.

Divalent and trivalent cations of iron and manganese play an important role in constraining the colour attributes of glass. Consequently, this important parameter must have been taken into consideration by ancient glassmakers, and provides insights into the reconstruction of the material culture of glass.

ACKNOWLEDGMENTS

G.E. Gigante and M. Martini are thanked for their helpful reviews. This research was supported by a F.A.R. grant from the University of Pavia.

REFERENCES

ABIDI N., DEROIDE B. and ZANCHETTA J. (1997) — *The interaction of Mn^{2+} with porous silica xerogels and the hydration-dehydration processes in the xerogels.* J. Non-Cryst. Solids, **221**, 59-69.

AMREIN H., BURKHARDT A. and STERN W.B. (1995) — *Analisen von Glasern aus der frukaiserzeitlichen Glaswerkstatt von aventicum (Schweiz).* Bull. Ass. Pro Aventico, **37**, 189-201.

BLAKE H. and MACCABRUNI C. (1985) — *Lo scavo a Villa Maria di Lomello (Pavia) 1984.* Archeologia Medievale, **XII**, 5-28.

BLAKE H., MACCABRUNI C. and PEARCE M. (1987) — *Ricerche archeologiche a Lomello 1984-85.* Archeologia Medievale, **XIV**, 157-87.

BRILL R.H. (1992) — *Chemical analyses of some glass from Frattesina.* J. of Glass Studies, **34**, 11-22.

BRILL R.H. (1999) — *Chemical analyses of early glass.* The Corning Museum of Glass, 2 (Tables of Analyses), 553 p.

CESANA A., CUOMO DI CAPRO N., MASSABO B. and TERRANI M. (1996) — *Analisi XRF in dispersione di energia su campioni vitrei provenienti da Albenga.* In «Atti 2e Giornate Nazionali di Studio AIHV», Comitato Nazionale Italiano, 147-55.

CHIAVARI C., MARTINI M., SIBILIA E., AZZONI C.B., DI MARTINO D. and VANDINI M. (2001) — *A study of ancient mosaic glass from the Mediterranean area.* Submitted to Archaeometry.

FIORI C. and MACCHIAROLA M. (1996) — *Studio e confronti fra la composizione chimica di vetri del II-I secolo a.C. provenienti da Delos (Grecia) e vetri provenienti dalla Capitanata (FG): Herdonia, I-II secolo d-C., Arpi e Ascoli Satriano, II secolo d.C.* In «Atti 2e Giornate Nazionali di Studio AIHV», Comitato Nazionale Italiano, 139-146.

GRATUZE B., SOULIER I. and BARRANDON J.N. (1997) — *L'analyse chimique, un outil au service de l'histoire du verre.* Verre, **3**, 31-43.

GRISCOM D.L. (1980) — *Electron spin resonance in glass.* J. Non-Cryst. Solids, **40**, 211-272.

MESSIGA B. and RICCARDI M.P. (2001) — *A petrological approach to the study of ancient glass.* Per. Mineral., **70**, 57-70.

MORETTI C. (2000) — *Provenienza e datazione dei vetri archeologici. Problematiche e prospettive date dall'utilizzo di nuove tecniche di indagine.* In «Atti I Congresso Nazionale di Archeometria», Verona 1999, 467-481.

NEWTON R. and DAVISON S. (1989) — Conservation of Glass. Butterworth and Heinemann, Oxford, 318 pp.

RUFFINI A., FIORI C. and VANDINI M. (1999a) — *Caratterizzazione dei vetri musivi antichi. Parte 1: metodologie d'analisi e risultati.* Ceramurgia, **XXIX-4**, 285-98.

RUFFINI A., FIORI C. and VANDINI M. (1999b) — *Caratterizzazione dei vetri musivi antichi. Parte 2: elaborazione dei dati analitici.* Ceramurgia, **XXIX 5-6**, 361-8.

SELLNER C. (1977) — *Untersuchungen an Waldglasern mit Elektronen-spinresonanz.* CVMA News Letter, **26**, Abs n° 298.

SELLNER C.H.J. and CAMARA B. (1979) — *Untersuchungen alter Glaser (Waldglas) auf Zussamenhang von Zusammensetzung, Farbe und Schmelzatmospare mit der Elektronenspektroscopie und der Elektronenspinresonanz (ESR).* Glastechn. Ber, **52,** 255-64.

TRISCARI M., QUARTIERI S., BOSCHERINI F. and SANI A. (2000) — *Application of X-ray Absorption Spectroscopy with synchrotron radiation to the study of glasses of archaeological interest.* In «Atti I Congresso Nazionale di Archeometria», Verona 1999, 459-466.